NeuroImage: Clinical 51 (2026) 104031

Contents lists available at ScienceDirect

NeuroImage: Clinical

journal homepage: www.elsevier.com/locate/ynicl

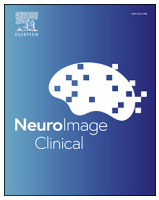

Predicting pattern and spread of brain atrophy and tau deposition in progressive supranuclear palsy

Alma Ghirelli [a,b,c,d], Farwa Ali [a], Yehkyoung C. Stephens [a], Heather M. Clark [a], Julie A.G. Stierwalt [a], Mary M. Machulda [e], Federica Agosta [b,c,d], Massimo Filippi [b,c,d,g,h], Dennis W. Dickson [i], Val J. Lowe [f], Keith A. Josephs [a], Jennifer L. Whitwell [f,*], Ryota Satoh [f]

[a] Department of Neurology, Mayo Clinic, Rochester, MN, USA
[b] Neuroimaging Research Unit, Division of Neuroscience, IRCCS San Raffaele Scientific Institute, Via Olgettina, 60, 20132 Milan, Italy
[c] Neurology Unit, IRCCS San Raffaele Scientific Institute, Milan, Italy
[d] Vita-Salute San Raffaele University, Milan, Italy
[e] Department of Psychiatry and Psychology, Mayo Clinic, Rochester, MN, United States
[f] Department of Radiology, Mayo Clinic, Rochester, MN 55905, USA
[g] Neurorehabilitation Unit, IRCCS San Raffaele Scientific Institute, Milan, Italy
[h] Neurophysiology Service, IRCCS San Raffaele Scientific Institute, Milan, Italy
[i] Department of Neuroscience, Mayo Clinic, Jacksonville, FL 32224, USA

ARTICLE INFO

Keywords:
PSP
Tau PET
MRI
Atrophy
Machine learning

ABSTRACT

Background: Progressive supranuclear palsy (PSP) is a 4-repeat tauopathy characterized by clinicopathological heterogeneity. The complex interplay between tau deposition, structural changes, and disease spread are unclear.
Objectives: To investigate the temporospatial patterns of tau propagation and neurodegeneration using multimodal imaging with MRI and flortaucipir (FTP) PET, and determine relationship with clinical heterogeneity.
Methods: 150 PSP patients (n = 66 Richardson's syndrome [PSP-RS], n = 26 parkinsonism [PSP-P], n = 25 speech-language [PSP-SL], n = 13 progressive gait freezing (PSP-PGF), n = 10 corticobasal syndrome [PSP-CBS], n = 3 frontal, n = 1 oculomotor and n = 6 postural instability) underwent 3 T-MRI and FTP-PET. Forty-three patients died and underwent autopsy. Subtype and Stage Inference (SuStaIn), an unsupervised machine learning algorithm that separates data-driven disease phenotypes distinguished by diverse temporal progression patterns, was applied to both MRI and FTP-PET W-scores (adjusted for age, sex and scanner, using 102 controls). Longitudinal MRI (n = 76) and FTP (n = 56) data, analysed with linear mixed models, were used to assess regional progression patterns and compared with the machine learning predictions.
Results: Two subtypes emerged across modalities. Subtype 1 exhibited initial subcortical involvement, mainly included PSP-RS and PSP-P patients and mostly featured PSP pathology, while subtype 2 exhibited early cortical involvement, PSP-SL patients and CBD pathology. FTP-PET stages preceded MRI stages, suggesting tau deposition anticipates atrophy. MRI stages were better in capturing clinical progression and predicting longitudinal disease evolution.
Conclusions: These findings suggest the existence of subcortical and cortical subtypes of PSP, with distinct clinicopathological features. Tau PET and MRI provide complementary insights into disease progression, with MRI more closely reflecting clinical evolution.

1. Introduction

Progressive Supranuclear Palsy (PSP) is a neurodegenerative disease characterized by the accumulation of 4R tau (Hauw et al., 1994). Clinically, PSP presents with ocular motor dysfunction, postural instability, akinesia, and cognitive dysfunction, although different variants have been recognized (Höglinger et al., 2017a; Respondek et al., 2014): PSP with Richardson's syndrome (PSP-RS), PSP with predominant corticobasal syndrome (PSP-CBS), PSP with predominant speech/language disorder (PSP-SL), PSP with predominant parkinsonism (PSP-P), PSP

* Corresponding author at: Professor of Radiology, Mayo Clinic, 200 1st St SW, Rochester, MN, USA.
E-mail address: whitwell.jennifer@mayo.edu (J.L. Whitwell).

https://doi.org/10.1016/j.nicl.2026.104031
Received 21 February 2026; Received in revised form 11 June 2026; Accepted 1 July 2026
Available online 2 July 2026

with predominant frontal presentation (PSP-F), PSP with progressive gait freezing (PSP-PGF), PSP with predominant postural instability (PSP-PI) and PSP with predominant ocular motor dysfunction (PSP-OM). These cortical and subcortical variants are distinguished by distinct structural and neuropathological features. Indeed, PSP-RS is characterized by a greater overall tau burden compared with PSP-P and PSP-PGF (Sakae et al., 2019), while PSP-F shows increased tau deposition in frontal and temporal regions (Sakae et al., 2019). PSP-CBS demonstrates a relative shift of tau pathology toward cortical areas, possibly reflecting overlap with corticobasal degeneration pathology (Ling et al., 2014; Tsuboi et al., 2005). In contrast, PSP-PGF is associated with minimal cortical tau pathology and predominant degeneration of subcortical structures, including the globus pallidus, substantia nigra, and subthalamic nucleus (Ahmed et al., 2008). While these clinical variants commonly result from PSP pathology, other pathologies can be observed including corticobasal degeneration (CBD) (Ali et al., 2018; Dickson et al., 2011; Respondek et al., 2014). This contributes to marked heterogeneity in both clinical presentation and pathological findings. Moreover, pathological tau accumulation begins during a preclinical phase and progresses variably across individuals. As a result, patients assessed at a single time point may represent different stages of a continuously evolving disease process.

Previous PSP studies analyzing biomarkers like MRI atrophy or tau PET uptake have often assumed either that patients share a common stage of tau accumulation (Grijalva et al., 2022; Whitwell et al., 2020), or that they exhibit a uniform clinical phenotype with similar disease progression (Agosta et al., 2018; Dutt et al., 2016). Yet, to reach a thorough biological understanding of the disease and appropriately stratify patients, it is important to consider the diversity of clinical groups alongside their individual progression trajectories. A recent post-mortem study has staged tau spread in different PSP syndromes and across different cell types (neurons, astrocytes, oligodendrocytes) and proposed the relative burden in those cell types as the key determinant of clinical variability. Indeed, early predominance of neuronal tau in the pallido-nigro-luysian system appears to define the classic subcortical trajectory, while greater astroglial or oligodendroglial tau involvement in motor cortical areas may characterize cortical variants (Kovacs et al., 2020). However, this staging was based on end-stage collected data. Temporal heterogeneity may be more efficiently captured ante-mortem using neuroimaging. Indeed, regional network architecture also plays a role: tau pathology appears to propagate preferentially along highly connected neural circuits, a phenomenon consistent with the cascading network failure model initially described in Alzheimer's disease and subsequently reported in PSP (Aghakhanyan et al., 2022; Jones et al., 2016). Understanding these pathogenic factors is essential not only for interpreting imaging-derived subtypes, but also for developing subtype-specific therapeutic strategies.

Patterns of atrophy on MRI and tau deposition detected by [18F] flortaucipir (FTP) PET have been well characterized in PSP (Grijalva et al., 2022; Whitwell et al., 2020). While all PSP variants exhibit volume loss and increased FTP uptake in key subcortical regions such as the striatum, globus pallidus, and thalamus, variability arises particularly in brainstem and cortical regions (Whitwell et al., 2020). PSP-RS prominently affects subcortical structures (midbrain, basal ganglia, superior cerebellar peduncle, thalamus) (Whitwell et al., 2017), while PSP-P and PSP-PGF affect mainly putamen and pallidum (Whitwell et al., 2020). Conversely, PSP-CBS, PSP-F, and PSP-SL show greater frontal involvement (Whitwell et al., 2020). These differences might indicate distinct spatiotemporal patterns of progression across clinical syndromes.

Capturing clinical and temporal heterogeneity in a cross-sectional setting would provide valuable insights into the underlying disease mechanisms, enabling precise patient classification and prognosis, and potentially reducing reliance on longitudinal data. Subtype and Stage Inference (SuStaIn) is a novel unsupervised machine learning algorithm designed to capture subtype and temporal heterogeneity using neuroimaging in a cross-sectional setting. The algorithm is fed by a set of biomarkers (e.g. regional volumes) and assigns subjects a probability of belonging to a given subtype and being at a given disease stage. While successfully applied in various neurodegenerative diseases (Saito et al., 2022; Young et al., 2021; Young et al., 2018; Zhou et al., 2023), its accuracy in estimating disease progression has not yet been validated with longitudinal data. Furthermore, while SuStaIn has been applied in PSP, most studies used T1-weighted MRI (Saito et al., 2022; Satoh et al., 2025; Scotton et al., 2023) and one study florzolotau PET data (Hong et al., 2023). No study has compared the efficacy of both MRI and tau PET in the same cohort of patients. This dual modality approach would allow a direct comparison of the temporospatial patterns of different, yet complementary, biomarkers of disease.

The aims of this study were (i) to apply SuStaIn to a heterogeneous cohort of PSP patients using both MRI and FTP PET to test the potential of both modalities to separate clinical subtypes and depict disease progression; (ii) explore how different pathologies distribute across different subtypes; (iii) evaluate SuStaIn accuracy in predicting disease trajectories by comparing patterns of progression with longitudinal data from a subset of the same cohort.

2. Methods

2.1. Participants

A total of 150 patients with a clinical diagnosis of PSP were recruited by the Neurodegenerative Research Group at Mayo Clinic (Rochester, MN) between February 2015 and January 2024. All patients underwent MRI on a 3 T scanner (either GE Medical or Siemens) and [18F] FTP tau PET as part of the same visit. Patients had a clinical diagnosis of PSP-RS ($n = 66$), PSP-P ($n = 26$), PSP-SL ($n = 25$), PSP-PGF ($n = 13$), PSP-CBS ($n = 10$), PSP-F ($n = 3$), PSP-OM (n = 1), and PSP-PI (n = 6). Diagnostic criteria were applied according to clinical judgment, adopting operational definitions previously outlined (Whitwell et al., 2019). Of 150 patients, forty-three died and underwent brain autopsy. We excluded the patients who had other pathological diagnoses than 4R tauopathies, such as multiple system atrophy (MSA).

Additionally, 102 controls who performed $\geq$23 at MoCA were enrolled. All participants provided informed consent in accordance with the Declaration of Helsinki. Study protocols were approved by the Mayo Clinic ethical committee. Further details on neurological and neuropsychological assessments are provided in Supplementary Materials.

A subset of patients underwent yearly follow-up. Longitudinal MRI data were available for 76 patients (22 patients had two follow-up scans, 8 had three scans, 2 had four scans, and 1 had six scans). Similarly, longitudinal FTP PET scans were available for 56 patients (17 having two follow-ups, six having three follow-ups, and one having four follow-ups). On average, scans were conducted one year apart. Disease duration from symptom onset was used as the time unit in the longitudinal analysis.

2.2. MRI and PET analysis

Details on MRI and PET analysis are provided in Supplementary materials and previous papers (Satoh et al., 2024; Satoh et al., 2025). Volumes and FTP uptake were calculated for 15 ROIs expected to present alterations in PSP (Whitwell et al., 2020). Nine subcortical ROIs included substantia nigra, dentate, subthalamic and red nucleus, pons, pallidum, caudate, putamen, and thalamus, while six cortical ROIs included prefrontal, precentral, supplementary motor cortex (SMA), occipital, temporal, and parietal cortex. Further details are available in Supplementary materials. We have visually evaluated the quality of MRI and PET processing for all participants, which included tissue segmentation, atlas alignment, and registration between MRI and PET images.

2.3. SuStaIn model

SuStaIn is an unsupervised machine learning algorithm that uses cross-sectional data to infer phenotypical (subtypes) and temporal heterogeneity (stages) (Young et al., 2018). SuStaIn reformulates the natural history of neurodegenerative diseases as a continuous linear accumulation of a given biomarker. In this study, we applied SuStaIn twice, once using regional volumes and once using regional FTP SUVRs. Volumes and FTP SUVR values were converted to W-scores, calculated as linear regression coefficients using age, sex and scanner, as covariates (MATLAB2022). Each W-score was calculated relative to a group of 102 controls, so the control population had a mean of 0 and a standard deviation of 1. No further adjustments were performed for FTP PET W-scores. Since MRI W-scores naturally become negative as atrophy progresses, they were inverted by multiplying them by minus one (W-scores increase as regional brain volumes decrease). Of note, W-scores were calculated for all available visits, but only baseline W-scores were included in the SuStaIn model. To find the optimal model, SuStaIn uses a hierarchical approach, initially fitted with a single subtype and then continuing to the predefined maximum number of subtypes. The advantage of a linear W-score model that reshapes the events to represent a gradual accumulation of a biomarker is that it does not necessitate knowledge about the timescale of change but uses each event as a control point of piecewise linear segments with flexible durations (Young et al., 2018). Further details on SuStaIn model are provided in Supplementary Materials.

To assess the influence of rare clinical variants ($n < 10$) on the SuStaIn models, we repeated the same SuStaIn analysis without PSP-PI ($n = 6$), PSP-F ($n = 3$), and PSP-OM ($n = 1$). Similarly, to assess the influence of CBD pathology, we also repeated the same SuStaIn analysis without patients with CBD ($n = 10$).

2.4. Neuropathological evaluation

Forty-three patients died and underwent brain autopsy. Each case was evaluated by an experienced neuropathologist according to current diagnostic methods (Ahmed et al., 2008; Dickson et al., 2002; Dickson et al., 2011; Josephs et al., 2006a; Lin et al., 2004; Sparaco et al., 1993; Whitwell et al., 2010). Nineteen patients died with PSP pathology, 10 with atypical PSP, 10 with CBD, three with MSA, and one with MELAS. This latter patient developed bilateral ischemic lesions and subdural hematoma one year after his last research follow-up, and none of these vascular alterations were present at the time of acquisitions implemented in this study.

2.5. Statistical analysis

Continuous variables were compared using Kruskal-Wallis, while categorical variables using chi-square tests. Correlations between SuStaIn stages and clinical scores were computed using Pearson's correlations. A p-value cutoff of 0.05 was set to determine statistical significance. Analyses were carried out with BlueSky Statistics v10.3.1 pro and MATLAB Statistics and Machine Learning Toolbox.

The lmer function from the lme4 package in R (4.5.3) was used to study longitudinal neuroimaging data. A linear mixed model was fitted using the maximum likelihood estimation method, in which the fixed effects coefficients represented the average change of each W-score associated with a unit change in disease duration, SuStaIn subtype, or their interaction after accounting for the random effect of individual patients. Linear regression models were plotted for each ROI for both modalities (MRI and FTP PET) and for each SuStaIn subtype. A qualitative visual comparison between the output of SuStaIn showing the predicted distribution of W-scores across stages and the actual longitudinal models was performed.

3. Results

3.1. FTP PET and MRI subtype and stage

A total of 145 patients were included in the SuStaIn analysis (Table 1). Four patients with a pathological diagnosis of MSA ($n = 3$) or MELAS ($n = 1$) were excluded. One patient was also excluded because an inaccurate atlas alignment was found during the visual assessment.

Two different patterns of progression emerged using FTP PET (Fig. 1A). SuStaIn subtype 1 ($n = 89$) presented early subcortical uptake, with involvement of the pallidum and red nucleus at stage 1 and involvement of the subthalamic nucleus, cerebellar dentate and putamen at stages 3–5. The thalamus, caudate and substantia nigra became involved by stage 9. The first cortical regions to become involved were the precentral gyrus and supplementary motor cortex which were involved by stage 13. Lastly, occipital, prefrontal, parietal, and temporal cortices showed mild involvement after approximately stage 20. In contrast, SuStaIn subtype 2 ($n = 25$) presented a more widespread and milder pattern of uptake, with early involvement of cortical and subcortical areas. The supplementary motor area, precentral cortex, and pallidum showed the greatest involvement at stage 1, followed by the parietal cortex and putamen. Uptake then progressed to involve most other regions with a mild and more homogeneous progressive pattern. Of note, 31 patients (21.4%) were not classified in any subtype and were considered stage 0 (i.e., uptake was insufficient to classify them).

Two patterns of progression also emerged with MRI (Fig. 1B). SuStaIn subtype 1 ($n = 106$) was similar to the FTP PET subtype 1 with a subcortical focus and early involvement of the pallidum and subthalamic nucleus at stage 1. The substantia nigra and red nucleus also showed mild involvement at stage 1 or 2, and the thalamus became involved at stage 7. The cerebellar dentate, putamen and caudate became involved at later stages than observed in the FTP SuStaIn subtype 1 and cortical regions did not become involved until after stage 20. MRI subtype 2 ($n = 37$) was also similar to the FTP PET subtype 1, with early involvement of the cortex, particularly the precentral cortex and supplementary motor area. In contrast to the FTP findings, the pallidum and putamen were not involved until later stages, while the substantia nigra, red nucleus and subthalamic nucleus showed mild involvement at earlier stages. Only two patients had a minimal degree of atrophy to be classified as Stage 0 and did not fit in any subtype. These two patients included one PSP-PGF patient with FTP subtype 0 (i.e., FTP Stage 0) and one PSP-SL patient with FTP subtype 2.

3.2. Clinical features and patient distribution across subtypes

Table 1 summarizes demographic and clinical features by SuStaIn subtypes. Across both modalities, most subtype 1 patients had a clinical diagnosis of PSP-RS, while subtype 2 was mainly driven by PSP-SL. Both FTP and MRI subtyping detected an increased prevalence of PSP in subtype 1 and atypical PSP and CBD in subtype 2. The number of patients who died at the time of the study was 79 for MRI-subtypes and 68 for FTP-subtypes. For both modalities, time from onset to death was significantly shorter in subtype 1. In neurological performances, subtype 1 showed higher (more abnormal) PSIS scores in both modalities. Dysarthria was more common in subtype 1. For MRI only, apraxia of speech (AOS) was more frequent in subtype 2, and subtype 2 patients had higher ASRS scores, indicating more severe AOS. No group differences emerged in AOS type (prosodic vs. phonetic).

Given the small sample sizes of rare variants (PSP-PI, $n = 6$; PSP-F, $n = 3$; PSP-OM, $n = 1$), we conducted a pre-specified sensitivity analysis repeating the full SuStaIn pipeline after excluding these three groups ($n = 10$ total). Results were highly consistent with those obtained in the full cohort (**Supplementary Figs. 4**), confirming that the inclusion of rare variants did not drive the identification of subtypes. Excluding patients with CBD pathology also preserved the two-subtype structure across both modalities, though the cortical subtype showed reduced robustness

Table 1
Clinical characteristics of PSP patients classified according to FTP PET subtypes.

	PSP cohort	FTP SuStaIn subtypes			MRI SuStaIn subtypes		
	***N* = 145**	**Subtype 1 (*N* = 89)**	**Subtype 2 (*N* = 25)**	**p-value**	**Subtype 1 (*N* = 106)**	**Subtype 2 (*N* = 37)**	**p-value**
Sex, Females N (%)	65 (45%)	36 (40%)	12 (48%)	0.50	49 (46%)	14 (38%)	0.38
Race, White/Caucasian N (%)	137 (94%)	84 (94%)	23 (92%)	0.66	101 (95%)	35 (95%)	0.87
Handedness, Right N (%)	122 (84%)	73 (82%)	23 (92%)	0.23	88 (83%)	32 (86%)	0.62
Age at Scan, years	71.1 (66.3, 76.1)	70.1 (65.2, 75.4)	72.8 (69.8, 77.3)	**0.04**	70.2 (65.4, 75.4)	74.1 (69.6, 79.0)	**0.007**
Age at onset, years	67.1 (61.0, 72.0)	65.4 (59.1, 70.6)	69.3 (64.9, 72.2)	0.08	65.6 (59.2, 70.8)	68.8 (63.9, 73.3)	**0.04**
Education	16 (12, 16)	16 (12, 16)	14 (12, 16)	0.26	16 (12, 16)	16 (12, 18)	0.66
Time from disease onset to death (years)	6.6 (5.3, 9.0)	6.1 (5.0, 8.8)	9.2 (6.2, 10.5)	**0.02**[1]	6.2 (5.0, 8.6)	8.6 (6.5, 10.4)	**0.007**[1]
Clinical diagnosis							
PSP-RS	66 (46%)	51 (57%)	5 (20%)		61 (58%)	5 (14%)	
PSP-P	22 (15%)	15 (17%)	3 (12%)		19 (18%)	3 (8%)	
PSP-PGF	12 (8%)	6 (7%)	2 (8%)		10 (9%)	1 (3%)	
PSP-PI	6 (4%)	1 (1%)	1 (4%)	**0.007**[2]	3 (3%)	3 (8%)	**<0.001**[2]
PSP-SL	25 (17%)	9 (10%)	10 (40%)		5 (5%)	19 (51%)	
PSP-CBS	10 (7%)	4 (4%)	3 (12%)		5 (5%)	5 (14%)	
PSP-F	3 (2%)	2 (2%)	1 (4%)		2 (2%)	1 (3%)	
PSP-OM	1 (1%)	1 (1%)	0 (0%)		1 (1%)	0 (0%)	
Pathological diagnosis							
PSP	19 (50%)	16 (76%)	1 (8%)		16 (80%)	3 (18%)	
Atypical PSP	9 (24%)	3 (14%)	5 (42%)	**<0.001**[2]	2 (10%)	6 (35%)	**<0.001**[2]
CBD	10 (26%)	2 (10%)	6 (50%)		2 (10%)	8 (47%)	
MoCA (/30)	24 (19, 26)	24 (19, 26)	23 (17, 27)	0.43[1]	24 (20, 26)	22 (17, 26)	0.07[1]
FAB (/18)	14 (12, 15)	14 (12, 16)	14 (9, 15)	0.62[1]	14 (12, 16)	13 (10, 15)	0.21[1]
BNT	14 (12, 14)	14 (12, 14)	13 (12, 15)	0.73[1]	14 (12, 14)	14 (12, 15)	>0.99[1]
TMT A	68 (50, 94)	62 (46, 88)	93 (55, 101)	0.16[1]	63 (48, 98)	75 (62, 93)	0.23[1]
TMT B	139 (105, 205)	137 (104, 180)	171 (135, 211)	0.15[1]	141 (104, 205)	130 (111, 205)	0.95[1]
PSP Rating Scale (/100)	36 (27, 45)	37 (28, 46)	37 (29, 52)	0.61[1]	36 (28, 44)	38 (27, 55)	0.43[1]
PSP Rating Scale gait-midline (/20)	12 (7, 15)	12 (7, 15)	13 (8, 16)	0.36[1]	12 (7, 14)	15 (6, 17)	0.28[1]
PSIS (/5)	3 (2, 4)	3 (2, 4)	2 (2,3)	**0.01**[1]	3 (2, 4)	2 (2, 3)	**0.04**[1]
UPDRS-III	38 (29, 52)	36 (25, 47)	43 (29, 54)	0.10[1]	37 (29, 48)	45 (26, 60)	0.07[1]
ASRS (/52)	4 (2, 8)	4 (2, 7)	4 (1, 8)	0.79[1]	4 (2, 6)	20 (2, 27)	**< 0.001**[1]
AOS (%)	33 (23%)	16 (18%)	7 (28%)	0.27[2]	11 (10%)	21 (57%)	**< 0.001**[2]
AOS type							
Phonetic	14 (42%)	7 (44%)	3 (43%)		3 (27%)	11 (52%)	
Prosodic	17 (52%)	9 (56%)	3 (43%)	0.29[2]	7 (64%)	9 (43%)	0.39[2]
Mixed	2 (6%)	0 (0%)	1 (14%)		1 (9%)	1 (5%)	
Dysarthria (%)	114 (79%)	77 (87%)	15 (60%)	**0.003**[2]	91 (86%)	22 (59%)	**0.001**[2]

Data shown as number (%), median (IQR). [1]Kruskal-Wallis rank sum test, [2]Pearson's Chi-squared test. Abbreviations: CBD: Corticobasal Degeneration; PSP: Progressive Supranuclear Palsy. PSP-CBS: PSP-Corticobasal Syndrome; PSP-F: PSP-Frontal; PSP-OM: PSP-Oculomotor dysfunction; PSP-P: PSP-Parkinsonism; PSP-PGF: PSP-Progressive gait freezing; PSP-PI: PSP-Postural instability; PSP-RS: PSP-Richardson's syndrome; PSP-SL: PSP-speech/language disorders. MoCA = Montreal Cognitive Assessment; PSIS=PSP Saccadic Impairment Scale; UPDRS = Unified Parkinson's Disease Rating Scale; ASRS = Apraxia of Speech Rating Scale; BNT: Boston Naming Test: TMT = Trail Making Test.

in FTP PET ($n = 5$ versus $n = 25$), reflecting the contribution of CBD cases to this pattern (**Supplementary Fig. 5**)."

To understand differences between the FTP PET and MRI results, we further examined cases classified differently by the two modalities. Details are reported in Supplementary materials.

3.3. Correlation between clinical progression and stages

FTP SuStaIn stages did not predict disease severity effectively, as most clinical measures showed no correlation with stage (Fig. 2). Significance emerged only when correlating TMT B and subtype 1 stages ($p = 0.01$, $r = 0.34$). MRI SuStaIn stages, instead, correlated well with disease severity (Fig. 3). MoCA scores declined with advancing stage in both subtypes, with a steeper decline in subtype 2. Similar findings were observed with the FAB. BNT scores did not correlate with stage in either subtype. TMT A and TMT B were associated with stage only in subtype 1. The PSP Rating Scale and PSIS correlated with stage in both subtypes. In contrast, MDS-UPDRS and ASRS scores did not change significantly with advancing stage.

3.4. Correlation between SuStaIn and longitudinal neuroimaging data

Lastly, we evaluated SuStaIn's ability to predict MRI and FTP PET disease trajectories by comparing its cross-sectional stage projections with slopes from linear mixed models derived from longitudinal data. Patients were categorized by SuStaIn subtype, and disease duration was included as a covariate. Slopes were qualitatively compared to assess how well SuStaIn captured progression. **Supplementary Fig. 3** shows SuStaIn-predicted FTP PET stage progression (left panels) versus actual longitudinal W-score trajectories (right panels). Longitudinal W-scores refer to values derived from real follow-up data. Overall, SuStaIn had limited accuracy in predicting longitudinal W-score changes: while SuStaIn models forecasted worsening W-scores across all ROIs, actual longitudinal data did not consistently support this. In subtype 1, SUVR values showed minimal change over time, resulting in relatively stable W-scores across cortical and subcortical regions. In subtype 2, observed data more closely matched SuStaIn predictions, showing a general positive trend in SUVR (**Supplementary Fig. 3 A–D, F, H—K, M–P**), though the magnitude of change was smaller than projected.

SuStaIn performed better with MRI data. In subtype 1, longitudinal W-scores showed consistent increases in subcortical regions—putamen, thalamus, pallidum, subthalamic nucleus, cerebellar dentate, substantia

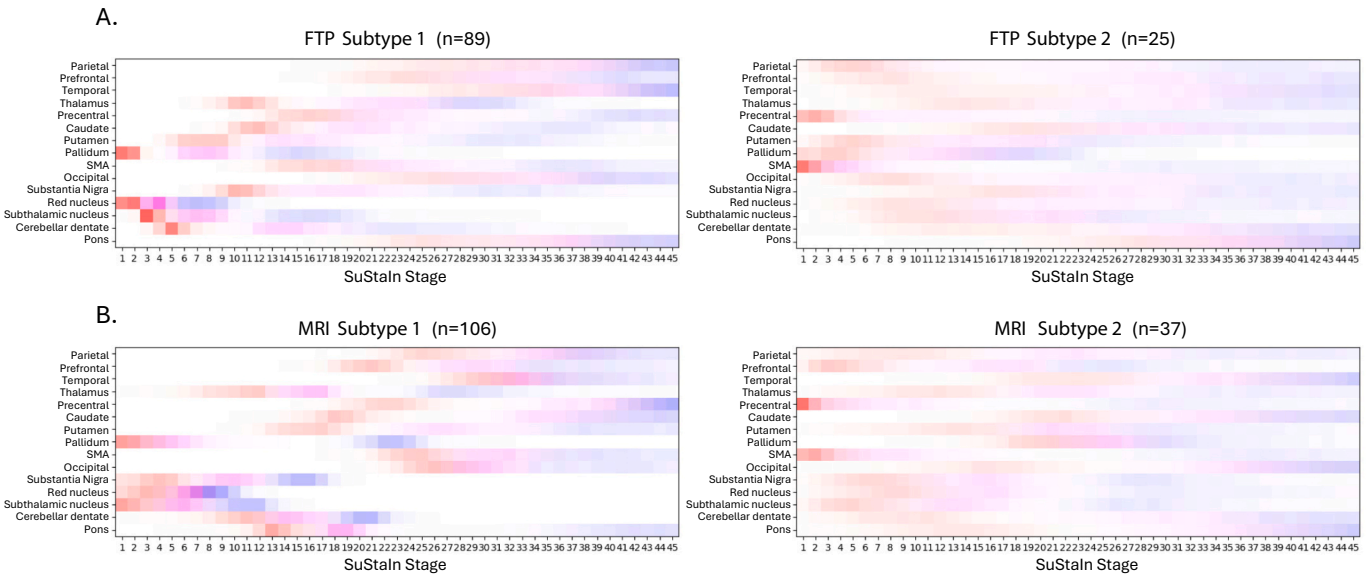

Fig. 1. Positional variance diagrams estimated by SuStaIn according to FTP PET (A) and MRI (B) data. The color of each region indicates the severity of tau uptake, which ranges from red (most severely involved) to magenta to blue (least severely involved).

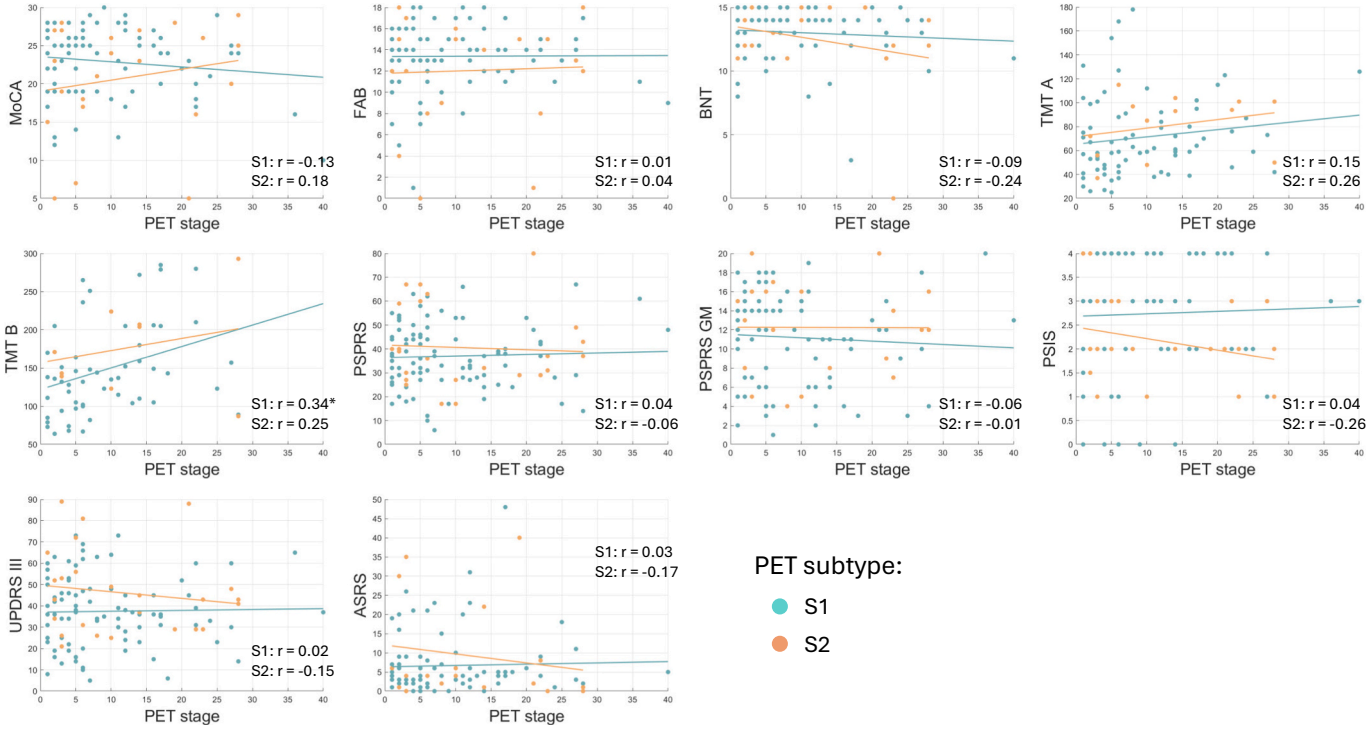

Fig. 2. Correlation between clinical test scores and SuStaIn stages across FTP PET subtypes. Each dot represents a subject. Subtype 1 = blue; subtype 2 = orange. Asterisks indicate *p*-values as $*p < 0.05$. MoCA = Montreal cognitive assessment; FAB=Frontal assessment battery; BNT = Boston naming test; TMT = Trail making test; PSPRS = Progressive supranuclear palsy rating scale; PSPRS-GM = PSP Rating Scale gait-midline; PSIS=PSP saccadic impairment scale; UPDRS = Unified Parkinson's disease rating scale; ASRS = Apraxia of speech rating scale.

nigra, and red nucleus—closely matching SuStaIn's predicted progression (Fig. 4; **F, G, H, J, L, M, P**). For subtype 2, longitudinal W-scores in all cortical regions increased more steeply than in subtype 1 (Fig. 4; **A, B, C, D, I, K**), reflecting the cortical-dominant pattern predicted by the model. In subcortical regions, subtype 2 also showed rising W-scores, aligning with SuStaIn projections in most areas, including the putamen, thalamus, pallidum, subthalamic nucleus, substantia nigra, and pons (Fig. 4; **F, G, H, J, M, O**).

4. Discussion

This study assessed spatiotemporal patterns of disease spread in PSP using both MRI and FTP PET. Both modalities identified two distinct subtypes—a subcortical and a cortical pattern—each associated with different clinical presentations and outcomes. The subcortical subtype was linked to shorter survival and PSP-RS phenotype, while the cortical subtype was rich in PSP-SL and CBD. MRI stages were more strongly associated with clinical measures and longitudinal change, suggesting

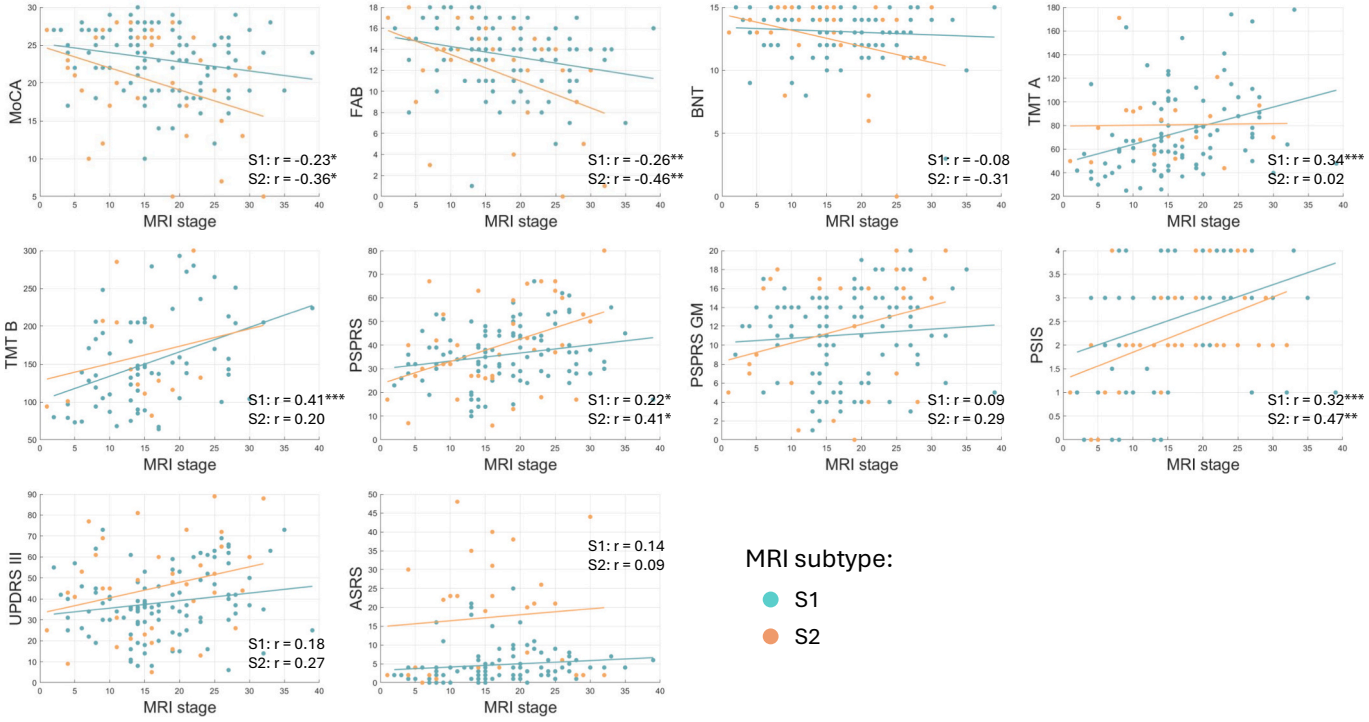

Fig. 3. Correlation between clinical test scores and SuStaIn stages across MRI subtypes. Each dot represents a subject. Subtype 1 = blue; subtype 2 = orange. Asterisks indicate p-values as *p < 0.05, **p < 0.01, and ***p < 0.01. MoCA = Montreal cognitive assessment; FAB=Frontal assessment battery; BNT = Boston naming test; TMT = Trail making test; PSPRS = Progressive supranuclear palsy rating scale; PSPRS-GM = PSP Rating Scale gait-midline; PSIS=PSP saccadic impairment scale; UPDRS = Unified Parkinson's disease rating scale; ASRS = Apraxia of speech rating scale.

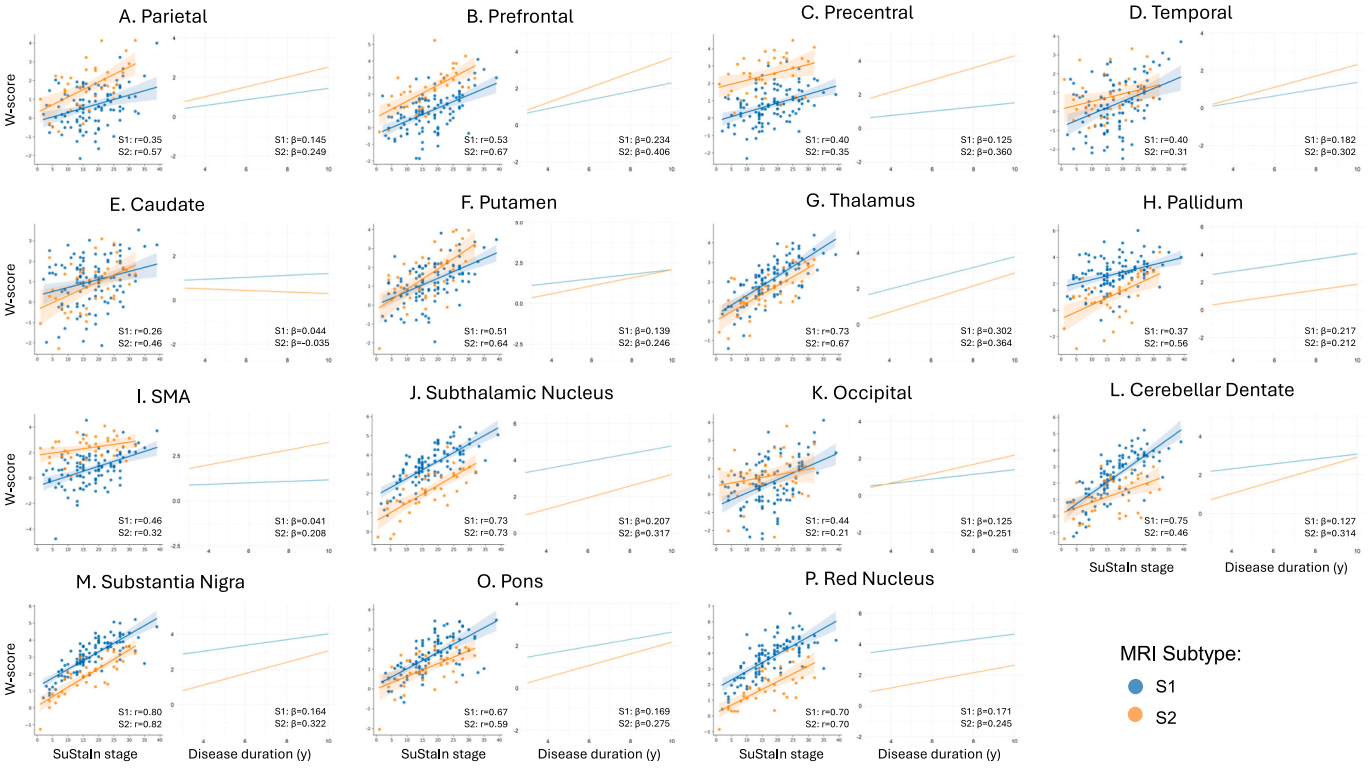

Fig. 4. Comparison of MRI disease progression predicted by SuStaIn versus longitudinal data models. Cross-sectional SuStaIn projections across subtypes (left) are compared to linear mixed models derived from actual longitudinal data (right) per each ROI. Fitted lines from the linear mixed effects model are shown between 3 and 10 years. Subtype 1 = blue; subtype 2 = orange. SMA = Supplementary motor area.

better utility for tracking disease evolution. FTP PET stages, while less predictive of clinical severity, appeared to precede MRI stages in several

regions, indicating that tau pathology may anticipate structural decline.

In both MRI and FTP data, subtype 1 followed a progression beginning in the pallidum and red nucleus, then involving subthalamic nucleus and later the thalamus. FTP PET revealed earlier involvement of subcortical (cerebellar dentate, putamen, caudate) and cortical (precentral cortex, SMA) regions. In contrast, atrophy and tau deposition in parietal, prefrontal, and occipital regions occurred more synchronously. These findings support the hypothesis that tau deposition leads to neuronal loss and neurodegeneration. Our group has previously found that the burden of combined neuronal and glial 4R tau in the striatum is relatively higher compared to the degree of volume loss in PSP-RS (Orlandi et al., 2024), possibly explaining why uptake on FTP PET in the striatum occurs earlier than atrophy. Furthermore, a positive correlation was previously demonstrated between FTP uptake and atrophy in the cerebellar dentate, red nucleus, and subthalamic nucleus, supporting a possible causal relationship between tau accumulation and subsequent tissue loss (Sintini et al., 2019). Contrasting with these findings, the substantia nigra showed early volume loss compared to FTP uptake. This mismatch may be driven by the fact that FTP uptake is influenced by reduced neuromelanin levels (Marquié et al., 2017).

Our findings align closely, though not exactly, with previous SuStaIn results by Scotton et al. (Scotton et al., 2023) who identified a cortical and a subcortical PSP pattern using MRI alone. Unlike their study, where midbrain atrophy appeared early in both subtypes, we found early midbrain involvement only in subtype 1. Our work suggests two different disease epicenters: midbrain for subcortical PSP and prefrontal cortex for cortical PSP. Similarly, Hong et al. (Hong et al., 2023) adopted a new-generation tau tracer ([18F] Florzolotau), also identifying similar subtypes with early tau uptake in subcortical regions for subtype 1 and simultaneous cortical-subcortical progression in subtype 2. Our study is distinctive in applying both PET and MRI SuStaIn within the same PSP cohort, providing unique insights into how tau deposition and atrophy progression patterns relate. The differential tau deposition observed between our subcortical subtype — predominantly comprising PSP-RS and PSP-P patients — and the cortical subtype is consistent with a recent review by Alster et al. (2025), who highlighted that tau neuroimaging yields differing results across PSP subtypes and that the pattern of tau accumulation depends critically on cell-type tropism. Importantly, it is emphasized that in vivo evaluation of tau accumulation by PET may ultimately redefine therapeutic stratification, an aspiration directly supported by the data-driven subtype framework presented here (Alster et al., 2025).

A neuropathology paper by Kovacs et al. (Kovacs et al., 2020) has recently described the distribution patterns of tau pathology in PSP, using postmortem data and applying conditional probability to model the sequential distribution of tau deposition. Our findings only partially corroborate their results. Their proposed progression starts with tau accumulation in the pallidum, subthalamic nucleus, and substantia nigra, followed by the tegmentum, pons, and striatum, then the dentate nucleus and amygdala, and finally the cortex—frontal first, then parietal and temporal, and lastly occipital. This pattern closely resembles our subtype 1 progression, particularly the early involvement of the pallidum and subthalamic nucleus, with the precentral cortex as the first cortical region affected. However, a key difference emerges in that Kovacs et al. suggest a single epicenter—the pallidum—for all PSP cases. In contrast, our SuStaIn model identifies two distinct epicenters: subcortical for subtype 1 and cortical (SMA and precentral cortex) for subtype 2. While the pallidum is involved early in both subtypes, FTP uptake in subtype 2 begins most prominently in motor-related cortical regions, diverging from the uniform model proposed by Kovacs. We argue that postmortem studies might miss early disease stages, where tau distribution likely differs between cortical and subcortical PSP subtypes. After death, tau has likely already accumulated in neocortical and subcortical regions, missing nuances characterizing early distribution. Autopsy data showed that MRI-defined subtypes correlated with pathology: subtype 1 patients mostly died with PSP, while subtype 2 with CBD or atypical PSP. Previous studies showed a predominance of PSP pathology in PSP-RS cases and CBD pathology in PSP-SL cases (Ali et al., 2019; Hokelekli et al., 2022; Orlandi et al., 2024). A similar distribution of pathology across subtypes was observed in the FTP-defined subtypes. These findings suggest MRI-based and FTP-based SuStaIn may help predict underlying 4R tauopathy, pending validation in external cohorts. Notably, patient selection in this study was based on clinical judgment, without prior knowledge of underlying pathology. We only excluded non-4R tauopathies such as MELAS and MSA to improve the model's reliability. We chose this clinically driven approach to reflect real-world conditions, as SuStaIn is intended to support prognosis in routine practice, where pathological confirmation is unavailable.

Clinical differences were observed across MRI and FTP-defined subtypes. Subtype 1, which included more PSP-RS patients, showed greater ocular motor impairment, more frequent dysarthria, and shorter survival—consistent with known features of PSP-RS (Clark et al., 2021). Subtype 2, with more PSP-SL and PSP-CBS cases, showed higher AOS prevalence and severity, and trends toward lower MoCA scores, reflecting greater cognitive and language deficits (Pavone et al., 2023). Although no formal survival analysis was performed, subtype 1 patients had shorter time from onset to death, aligning with previous studies linking PSP-RS to worse prognosis (Guasp et al., 2021), secondary to cognitive impairment, frequent falls (Agarwal and Gilbert, 2024) and early-onset dysphagia (Glasmacher et al., 2017).

Only MRI-based SuStaIn stages reliably tracked clinical progression in PSP. They correlated with worsening MoCA, FAB, PSP Rating Scale, and PSIS scores in both subtypes, and with declines in executive function and processing speed (TMT A and B) in subtype 1. These results suggest that neurodegeneration measured by MRI better reflects clinical deterioration than tau burden captured by FTP PET.

SuStaIn's predictions of FTP PET disease progression did not align well with actual longitudinal data. We previously demonstrated that FTP uptake increases over one year in the pallidum, precentral cortex, cerebellar dentate, and midbrain in PSP-RS; however, these longitudinal changes did not correlate with clinical severity and were less robust than MRI-based measures, reinforcing the superior reliability of MRI in tracking disease progression (Whitwell et al., 2019). The lack of consistent longitudinal findings in FTP could reflect variability in individual trajectories, potential limitations in FTP's sensitivity to 4R tau (Ghirelli et al., 2020; Lowe et al., 2016; Sander et al., 2016), and possible biological factors—such as concurrent neurodegeneration that scavenges tau accumulation (Sato et al., 2018) or declining glial tau with disease progression (Josephs et al., 2006b). Notwithstanding the lower sensitivity of flortaucipir for 4R tau compared to AD-related 3R + 4R tau, the fact that Hong et al. (Hong et al., 2023) found similar subtype patterns using the more sensitive tracer florzolotau reinforces the validity of our findings. This lower affinity may contribute to underestimation of tau burden in some PSP patients, particularly in early stages or in regions with low tau density. Despite these limitations, the consistency of subtype patterns across tracers suggests that the biological subtypes identified reflect meaningful differences in disease expression.

MRI, on the other hand, outperformed FTP PET in predicting disease trajectories. This aligns with prior longitudinal MRI studies in PSP-RS that reported widespread cortical and subcortical atrophy (Josephs et al., 2013). One such study found that midbrain, frontal lobes, and third ventricle volumes were especially sensitive markers, capable of detecting significant annualized changes with relatively small sample sizes. In our cohort, the widespread decline in volume likely reflects the longer follow-up period (Höglinger et al., 2017b). We also acknowledge that visual comparison is a qualitative approach and does not offer a rigorous statistical assessment of SuStaIn's precision in modeling longitudinal progression, limiting the strength of conclusions drawn from this comparison.

Beyond their scientific interest, the subtypes identified here carry direct clinical relevance. First, subtype assignment at baseline — achievable from a single cross-sectional imaging session — may assist

clinicians in anticipating disease trajectory and counselling patients and families regarding prognosis. Subtype 1 patients showed shorter time from onset to death and greater ocular motor impairment, consistent with the known aggressive course of PSP-RS. Subtype 2 patients showed greater speech and language involvement and trends toward lower MoCA scores, pointing toward distinct management needs, including early speech-language therapy. Second, and perhaps most critically for the field, accurate subtyping and staging of PSP patients at baseline has important implications for clinical trial design. The failure of several recent PSP therapeutic trials may in part reflect biological heterogeneity within enrolled populations (Dam et al., 2021; Höglinger et al., 2021). Stratifying patients by imaging-derived subtype prior to trial entry could enrich study populations with individuals sharing a common disease trajectory, increasing sensitivity to detect treatment effects. Third, the observation that MRI-based SuStaIn stages reliably track clinical progression — while FTP PET stages do not — has immediate practical implications: MRI staging may be more suitable as a trial endpoint or progression biomarker in PSP, at least with currently available tau tracers.

Several limitations should be acknowledged. The autopsy subset ($n = 43$) is relatively small, and pathological validation of imaging subtypes should be considered preliminary pending external replication. FTP's substantially lower affinity for 4R tau may have attenuated PET-derived signals, though the consistency of our subtype structure with a study (Hong et al., 2023) using the higher-affinity [18F]Florzolotau tracer argues against a tracer artifact. SuStaIn infers trajectories from cross-sectional data without explicit temporal information, and our comparison with longitudinal data was qualitative rather than formally validated. Finally, single-center recruitment at a tertiary referral center and the predominantly Caucasian cohort composition (95%) may limit generalizability of the findings.

In summary, SuStaIn proved to be a valuable tool for predicting atrophy patterns over time and discerning diverse neurodegeneration trajectories in PSP, correlating accurately with disease severity scales. However, its application with FTP PET data requires caution, as longitudinal predictions are less precise and correlate poorly with clinical severity measures. Despite this, tools capable of predicting longitudinal progression solely from cross-sectional data could significantly assist clinicians in patient prognosis and appropriate clinical trial inclusion.

CRediT authorship contribution statement

Alma Ghirelli: Writing – original draft, Visualization, Validation, Methodology, Investigation. **Farwa Ali:** Writing – review & editing, Resources. **Yehkyoung C. Stephens:** Writing – review & editing, Resources. **Heather M. Clark:** Writing – review & editing, Resources. **Julie A.G. Stierwalt:** Writing – review & editing, Resources. **Mary M. Machulda:** Writing – review & editing, Resources. **Federica Agosta:** Writing – review & editing, Supervision. **Massimo Filippi:** Writing – review & editing, Supervision. **Dennis W. Dickson:** Writing – review & editing, Resources. **Val J. Lowe:** Writing – review & editing, Resources. **Keith A. Josephs:** Writing – review & editing, Supervision, Resources, Project administration, Methodology, Funding acquisition, Conceptualization. **Jennifer L. Whitwell:** Writing – review & editing, Supervision, Resources, Project administration, Methodology, Funding acquisition, Conceptualization. **Ryota Satoh:** Writing – review & editing, Software, Methodology, Investigation.

Funding

This study was funded by National Institutes of Health grant R01-NS89757, RF1-NS112153.

Declaration of competing interest

The authors declare that they have no known competing financial interests or personal relationships that could have appeared to influence the work reported in this paper.

Acknowledgment

We thank all the patients and their families for their commitment to the research.

Appendix A. Supplementary data

Supplementary data to this article can be found online at https://doi.org/10.1016/j.nicl.2026.104031.

Data availability

The data that support the findings of this study are available from the corresponding author, upon reasonable request.

References

Agarwal, S., Gilbert, R., 2024. Progressive supranuclear palsy. StatPearls, Treasure Island (FL). . StatPearls publishing copyright © 2024, StatPearls publishing LLC.,.

Aghakhanyan, G., Rullmann, M., Rumpf, J., Schroeter, M.L., Scherlach, C., Patt, M., Brendel, M., Koglin, N., Stephens, A.W., Classen, J., Hoffmann, K.T., Sabri, O., Barthel, H., 2022. Interplay of tau and functional network connectivity in progressive supranuclear palsy: a [(18)F]PI-2620 PET/MRI study. Eur. J. Nucl. Med. Mol. Imaging 50, 103–114.

Agosta, F., Caso, F., Ječmenica-Lukić, M., Petrović, I.N., Valsasina, P., Meani, A., Copetti, M., Kostić, V.S., Filippi, M., 2018. Tracking brain damage in progressive supranuclear palsy: a longitudinal MRI study. J. Neurol. Neurosurg. Psychiatry 89, 696–701.

Ahmed, Z., Josephs, K.A., Gonzalez, J., DelleDonne, A., Dickson, D.W., 2008. Clinical and neuropathologic features of progressive supranuclear palsy with severe pallido-nigro-luysial degeneration and axonal dystrophy. Brain 131, 460–472.

Ali, F., Whitwell, J.L., Martin, P.R., Senjem, M.L., Knopman, D.S., Jack, C.R., Lowe, V.J., Petersen, R.C., Boeve, B.F., Josephs, K.A., 2018. [(18)F] AV-1451 uptake in corticobasal syndrome: the influence of beta-amyloid and clinical presentation. J. Neurol. 265, 1079–1088.

Ali, F., Martin, P.R., Botha, H., Ahlskog, J.E., Bower, J.H., Masumoto, J.Y., Maraganore, D., Hassan, A., Eggers, S., Boeve, B.F., Knopman, D.S., Drubach, D., Petersen, R.C., Dunkley, E.D., van Gerpen, J., Uitti, R., Whitwell, J.L., Dickson, D.W., Josephs, K.A., 2019. Sensitivity and specificity of diagnostic criteria for progressive supranuclear palsy. Mov. Disord. 34, 1144–1153.

Alster, P., van Eimeren, T., Madetko-Alster, N., 2025. Tau positron emission tomography in the Parkinson and Richardson subtypes of progressive supranuclear palsy. Parkinsonism Relat. Disord. 137, 107939.

Clark, H.M., Utianski, R.L., Ali, F., Botha, H., Whitwell, J.L., Josephs, K.A., 2021. Motor speech disorders and communication limitations in progressive supranuclear palsy. Am. J. Speech Lang. Pathol. 30, 1361–1372.

Dam, T., Boxer, A.L., Golbe, L.I., Höglinger, G.U., Morris, H.R., Litvan, I., Lang, A.E., Corvol, J.C., Aiba, I., Grundman, M., Yang, L., Tidemann-Miller, B., Kupferman, J., Harper, K., Kamisoglu, K., Wald, M.J., Graham, D.L., Gedney, L., O'Gorman, J., Haeberlein, S.B., 2021. Safety and efficacy of anti-tau monoclonal antibody gosuranemab in progressive supranuclear palsy: a phase 2, randomized, placebo-controlled trial. Nat. Med. 27, 1451–1457.

Dickson, D.W., Bergeron, C., Chin, S.S., Duyckaerts, C., Horoupian, D., Ikeda, K., Jellinger, K., Lantos, P.L., Lippa, C.F., Mirra, S.S., Tabaton, M., Vonsattel, J.P., Wakabayashi, K., Litvan, I., 2002. Office of Rare Diseases neuropathologic criteria for corticobasal degeneration. J. Neuropathol. Exp. Neurol. 61, 935–946.

Dickson, D.W., Kouri, N., Murray, M.E., Josephs, K.A., 2011. Neuropathology of frontotemporal lobar degeneration-tau (FTLD-tau). J. Mol. Neurosci. 45, 384–389.

Dutt, S., Binney, R.J., Heuer, H.W., Luong, P., Attygalle, S., Bhatt, P., Marx, G.A., Elofson, J., Tartaglia, M.C., Litvan, I., McGinnis, S.M., Dickerson, B.C., Kornak, J., Waltzman, D., Voltarelli, L., Schuff, N., Rabinovici, G.D., Kramer, J.H., Jack Jr., C.R., Miller, B.L., Rosen, H.J., Boxer, A.L., 2016. Progression of brain atrophy in PSP and CBS over 6 months and 1 year. Neurology 87, 2016–2025.

Ghirelli, A., Tosakulwong, N., Weigand, S.D., Clark, H.M., Ali, F., Botha, H., Duffy, J.R., Utianski, R.L., Buciuc, M., Murray, M.E., Labuzan, S.A., Spychalla, A.J., Pham, N.T. T., Schwarz, C.G., Senjem, M.L., Machulda, M.M., Baker, M., Rademakers, R., Filippi, M., Jack Jr., C.R., Lowe, V.J., Parisi, J.E., Dickson, D.W., Josephs, K.A., Whitwell, J.L., 2020. Sensitivity-specificity of tau and amyloid β positron emission tomography in frontotemporal lobar degeneration. Ann. Neurol. 88, 1009–1022.

Glasmacher, S.A., Leigh, P.N., Saha, R.A., 2017. Predictors of survival in progressive supranuclear palsy and multiple system atrophy: a systematic review and meta-analysis. J. Neurol. Neurosurg. Psychiatry 88, 402–411.

Grijalva, R.M., Pham, N.T.T., Huang, Q., Martin, P.R., Ali, F., Clark, H.M., Duffy, J.R., Utianski, R.L., Botha, H., Machulda, M.M., Weigand, S.D., Ahlskog, J.E., Dickson, D. W., Josephs, K.A., Whitwell, J.L., 2022. Brainstem biomarkers of clinical variant and pathology in progressive supranuclear palsy. Mov. Disord. 37, 702–712.

Guasp, M., Molina-Porcel, L., Painous, C., Caballol, N., Camara, A., Perez-Soriano, A., Sánchez-Gómez, A., Garrido, A., Muñoz, E., Marti, M.J., Valldeoriola, F., Grau, O., Gelpí, E., Respondek, G., Höglinger, G.H., Compta, Y., 2021. Association of PSP phenotypes with survival: a brain-bank study. Parkinsonism Relat. Disord. 84, 77–81.

Hauw, J.J., Daniel, S.E., Dickson, D., Horoupian, D.S., Jellinger, K., Lantos, P.L., McKee, A., Tabaton, M., Litvan, I., 1994. Preliminary NINDS neuropathologic criteria for Steele-Richardson-Olszewski syndrome (progressive supranuclear palsy). Neurology 44, 2015–2019.

Höglinger, G.U., Respondek, G., Stamelou, M., Kurz, C., Josephs, K.A., Lang, A.E., Mollenhauer, B., Müller, U., Nilsson, C., Whitwell, J.L., Arzberger, T., Englund, E., Gelpi, E., Giese, A., Irwin, D.J., Meissner, W.G., Pantelyat, A., Rajput, A., van Swieten, J.C., Troakes, C., Antonini, A., Bhatia, K.P., Bordelon, Y., Compta, Y., Corvol, J.C., Colosimo, C., Dickson, D.W., Dodel, R., Ferguson, L., Grossman, M., Kassubek, J., Krismer, F., Levin, J., Lorenzl, S., Morris, H.R., Nestor, P., Oertel, W.H., Poewe, W., Rabinovici, G., Rowe, J.B., Schellenberg, G.D., Seppi, K., van Eimeren, T., Wenning, G.K., Boxer, A.L., Golbe, L.I., Litvan, I., 2017a. Clinical diagnosis of progressive supranuclear palsy: the movement disorder society criteria. Mov. Disord. 32, 853–864.

Höglinger, G.U., Schöpe, J., Stamelou, M., Kassubek, J., Del Ser, T., Boxer, A.L., Wagenpfeil, S., Huppertz, H.J., 2017b. Longitudinal magnetic resonance imaging in progressive supranuclear palsy: a new combined score for clinical trials. Mov. Disord. 32, 842–852.

Höglinger, G.U., Litvan, I., Mendonca, N., Wang, D., Zheng, H., Rendenbach-Mueller, B., Lon, H.K., Jin, Z., Fisseha, N., Budur, K., Gold, M., Ryman, D., Florian, H., 2021. Safety and efficacy of tilavonemab in progressive supranuclear palsy: a phase 2, randomised, placebo-controlled trial. Lancet Neurol. 20, 182–192.

Hokelekli, F.O., Duffy, J.R., Clark, H.M., Utianski, R.L., Botha, H., Ali, F., Stierwalt, J.A., Machulda, M.M., Reichard, R.R., Dickson, D.W., Whitwell, J.L., Josephs, K.A., 2022. Autopsy validation of progressive supranuclear palsy-predominant speech/language disorder criteria. Mov. Disord. 37, 213–218.

Hong, J., Lu, J., Liu, F., Wang, M., Li, X., Clement, C., Lopes, L., Brendel, M., Rominger, A., Yen, T.C., Guan, Y., Tian, M., Wang, J., Zuo, C., Shi, K., 2023. Uncovering distinct progression patterns of tau deposition in progressive supranuclear palsy using [(18)F]Florzolotau PET imaging and subtype/stage inference algorithm. EBioMedicine 97, 104835.

Jones, D.T., Knopman, D.S., Gunter, J.L., Graff-Radford, J., Vemuri, P., Boeve, B.F., Petersen, R.C., Weiner, M.W., Jack Jr., C.R., 2016. Cascading network failure across the Alzheimer's disease spectrum. Brain 139, 547–562.

Josephs, K.A., Katsuse, O., Beccano-Kelly, D.A., Lin, W.L., Uitti, R.J., Fujino, Y., Boeve, B. F., Hutton, M.L., Baker, M.C., Dickson, D.W., 2006a. Atypical progressive supranuclear palsy with corticospinal tract degeneration. J. Neuropathol. Exp. Neurol. 65, 396–405.

Josephs, K.A., Mandrekar, J.N., Dickson, D.W., 2006b. The relationship between histopathological features of progressive supranuclear palsy and disease duration. Parkinsonism Relat. Disord. 12, 109–112.

Josephs, K.A., Xia, R., Mandrekar, J., Gunter, J.L., Senjem, M.L., Jack Jr., C.R., Whitwell, J.L., 2013. Modeling trajectories of regional volume loss in progressive supranuclear palsy. Mov. Disord. 28, 1117–1124.

Kovacs, G.G., Lukic, M.J., Irwin, D.J., Arzberger, T., Respondek, G., Lee, E.B., Coughlin, D., Giese, A., Grossman, M., Kurz, C., McMillan, C.T., Gelpi, E., Compta, Y., van Swieten, J.C., Laat, L.D., Troakes, C., Al-Sarraj, S., Robinson, J.L., Roeber, S., Xie, S.X., Lee, V.M., Trojanowski, J.Q., Höglinger, G.U., 2020. Distribution patterns of tau pathology in progressive supranuclear palsy. Acta Neuropathol. 140, 99–119.

Lin, W.L., DeLucia, M.W., Dickson, D.W., 2004. Alpha-synuclein immunoreactivity in neuronal nuclear inclusions and neurites in multiple system atrophy. Neurosci. Lett. 354, 99–102.

Ling, H., de Silva, R., Massey, L.A., Courtney, R., Hondhamuni, G., Bajaj, N., Lowe, J., Holton, J.L., Lees, A., Revesz, T., 2014. Characteristics of progressive supranuclear palsy presenting with corticobasal syndrome: a cortical variant. Neuropathol. Appl. Neurobiol. 40, 149–163.

Lowe, V.J., Curran, G., Fang, P., Liesinger, A.M., Josephs, K.A., Parisi, J.E., Kantarci, K., Boeve, B.F., Pandey, M.K., Bruinsma, T., Knopman, D.S., Jones, D.T., Petrucelli, L., Cook, C.N., Graff-Radford, N.R., Dickson, D.W., Petersen, R.C., Jack Jr., C.R., Murray, M.E., 2016. An autoradiographic evaluation of AV-1451 tau PET in dementia. Acta Neuropathol. Commun. 4, 58.

Marquié, M., Verwer, E.E., Meltzer, A.C., Kim, S.J.W., Agüero, C., Gonzalez, J., Makaretz, S.J., Siao Tick Chong, M., Ramanan, P., Amaral, A.C., Normandin, M.D., Vanderburg, C.R., Gomperts, S.N., Johnson, K.A., Frosch, M.P., Gómez-Isla, T., 2017. Lessons learned about [F-18]-AV-1451 off-target binding from an autopsy-confirmed Parkinson's case. Acta Neuropathol. Commun. 5, 75.

Orlandi, F., Carlos, A.F., Ali, F., Clark, H.M., Duffy, J.R., Utianski, R.L., Botha, H., Machulda, M.M., Stephens, Y.C., Schwarz, C.G., Senjem, M.L., Jack, C.R., Agosta, F., Filippi, M., Dickson, D.W., Josephs, K.A., Whitwell, J.L., 2024. Histologic tau lesions and magnetic resonance imaging biomarkers differ across two progressive supranuclear palsy variants. Brain Commun 6, fcae113.

Pavone, C., Weigand, S.W., Ali, F., Clark, H.M., Botha, H., Machulda, M.M., Savica, R., Pham, N.T.T., Grijalva, R.M., Schwarz, C.G., Senjem, M.L., Agosta, F., Filippi, M., Jack, C.R., Lowe, V.J., Josephs, K.A., Whitwell, J.L., 2023. Longitudinal clinical decline and baseline predictors in progressive supranuclear palsy. Parkinsonism Relat. Disord. 107, 105290.

Respondek, G., Stamelou, M., Kurz, C., Ferguson, L.W., Rajput, A., Chiu, W.Z., van Swieten, J.C., Troakes, C., Al Sarraj, S., Gelpi, E., Gaig, C., Tolosa, E., Oertel, W.H., Giese, A., Roeber, S., Arzberger, T., Wagenpfeil, S., Höglinger, G.U., 2014. The phenotypic spectrum of progressive supranuclear palsy: a retrospective multicenter study of 100 definite cases. Mov. Disord. 29, 1758–1766.

Saito, Y., Kamagata, K., Wijeratne, P.A., Andica, C., Uchida, W., Takabayashi, K., Fujita, S., Akashi, T., Wada, A., Shimoji, K., Hori, M., Masutani, Y., Alexander, D.C., Aoki, S., 2022. Temporal progression patterns of brain atrophy in Corticobasal syndrome and progressive supranuclear palsy revealed by subtype and stage inference (SuStaIn). Front. Neurol. 13, 814768.

Sakae, N., Josephs, K.A., Litvan, I., Murray, M.E., Duara, R., Uitti, R.J., Wszolek, Z.K., Graff-Radford, N.R., Dickson, D.W., 2019. Neuropathologic basis of frontotemporal dementia in progressive supranuclear palsy. Mov. Disord. 34, 1655–1662.

Sander, K., Lashley, T., Gami, P., Gendron, T., Lythgoe, M.F., Rohrer, J.D., Schott, J.M., Revesz, T., Fox, N.C., Årstad, E., 2016. Characterization of tau positron emission tomography tracer [(18)F]AV-1451 binding to postmortem tissue in Alzheimer's disease, primary tauopathies, and other dementias. Alzheimers Dement. 12, 1116–1124.

Sato, C., Barthélemy, N.R., Mawuenyega, K.G., Patterson, B.W., Gordon, B.A., Jockel-Balsarotti, J., Sullivan, M., Crisp, M.J., Kasten, T., Kirmess, K.M., Kanaan, N.M., Yarasheski, K.E., Baker-Nigh, A., Benzinger, T.L.S., Miller, T.M., Karch, C.M., Bateman, R.J., 2018. Tau kinetics in neurons and the human central nervous system. Neuron 97, 1284–1298.e1287.

Satoh, R., Ali, F., Botha, H., Lowe, V.J., Josephs, K.A., Whitwell, J.L., 2024. Direct comparison between (18)F-Flortaucipir tau PET and quantitative susceptibility mapping in progressive supranuclear palsy. Neuroimage 286, 120509.

Satoh, R., Sekiya, H., Ali, F., Clark, H.M., Utianski, R.L., Duffy, J.R., Machulda, M.M., Dickson, D.W., Josephs, K.A., Whitwell, J.L., 2025. Uncovering image-driven subtypes with distinct pathology and clinical course in autopsy-confirmed four repeat tauopathies. Ann. Neurol. 98, 492–507.

Scotton, W.J., Shand, C., Todd, E., Bocchetta, M., Cash, D.M., VandeVrede, L., Heuer, H., Young, A.L., Oxtoby, N., Alexander, D.C., Rowe, J.B., Morris, H.R., Boxer, A.L., Rohrer, J.D., Wijeratne, P.A., 2023. Uncovering spatiotemporal patterns of atrophy in progressive supranuclear palsy using unsupervised machine learning. Brain Commun 5, fcad048.

Sintini, I., Schwarz, C.G., Senjem, M.L., Reid, R.I., Botha, H., Ali, F., Ahlskog, J.E., Jack Jr., C.R., Lowe, V.J., Josephs, K.A., Whitwell, J.L., 2019. Multimodal neuroimaging relationships in progressive supranuclear palsy. Parkinsonism Relat. Disord. 66, 56–61.

Sparaco, M., Bonilla, E., DiMauro, S., Powers, J.M., 1993. Neuropathology of mitochondrial encephalomyopathies due to mitochondrial DNA defects. J. Neuropathol. Exp. Neurol. 52, 1–10.

Tsuboi, Y., Josephs, K.A., Boeve, B.F., Litvan, I., Caselli, R.J., Caviness, J.N., Uitti, R.J., Bott, A.D., Dickson, D.W., 2005. Increased tau burden in the cortices of progressive supranuclear palsy presenting with corticobasal syndrome. Mov. Disord. 20, 982–988.

Whitwell, J.L., Jack Jr., C.R., Boeve, B.F., Parisi, J.E., Ahlskog, J.E., Drubach, D.A., Senjem, M.L., Knopman, D.S., Petersen, R.C., Dickson, D.W., Josephs, K.A., 2010. Imaging correlates of pathology in corticobasal syndrome. Neurology 75, 1879–1887.

Whitwell, J.L., Lowe, V.J., Tosakulwong, N., Weigand, S.D., Senjem, M.L., Schwarz, C.G., Spychalla, A.J., Petersen, R.C., Jack Jr., C.R., Josephs, K.A., 2017. [(18) F]AV-1451 tau positron emission tomography in progressive supranuclear palsy. Mov. Disord. 32, 124–133.

Whitwell, J.L., Tosakulwong, N., Schwarz, C.G., Botha, H., Senjem, M.L., Spychalla, A.J., Ahlskog, J.E., Knopman, D.S., Petersen, R.C., Jack Jr., C.R., Lowe, V.J., Josephs, K. A., 2019. MRI outperforms [18F]AV-1451 PET as a longitudinal biomarker in progressive supranuclear palsy. Mov. Disord. 34, 105–113.

Whitwell, J.L., Tosakulwong, N., Botha, H., Ali, F., Clark, H.M., Duffy, J.R., Utianski, R. L., Stevens, C.A., Weigand, S.D., Schwarz, C.G., Senjem, M.L., Jack, C.R., Lowe, V.J., Ahlskog, J.E., Dickson, D.W., Josephs, K.A., 2020. Brain volume and flortaucipir analysis of progressive supranuclear palsy clinical variants. Neuroimage Clin 25, 102152.

Young, A.L., Marinescu, R.V., Oxtoby, N.P., Bocchetta, M., Yong, K., Firth, N.C., Cash, D. M., Thomas, D.L., Dick, K.M., Cardoso, J., van Swieten, J., Borroni, B., Galimberti, D., Masellis, M., Tartaglia, M.C., Rowe, J.B., Graff, C., Tagliavini, F., Frisoni, G.B., Laforce Jr., R., Finger, E., de Mendonça, A., Sorbi, S., Warren, J.D., Crutch, S., Fox, N.C., Ourselin, S., Schott, J.M., Rohrer, J.D., Alexander, D.C., 2018. Uncovering the heterogeneity and temporal complexity of neurodegenerative diseases with subtype and stage inference. Nat. Commun. 9, 4273.

Young, A.L., Bocchetta, M., Russell, L.L., Convery, R.S., Peakman, G., Todd, E., Cash, D. M., Greaves, C.V., van Swieten, J., Jiskoot, L., Seelaar, H., Moreno, F., Sanchez-Valle, R., Borroni, B., Laforce Jr., R., Masellis, M., Tartaglia, M.C., Graff, C., Galimberti, D., Rowe, J.B., Finger, E., Synofzik, M., Vandenberghe, R., de Mendonça, A., Tagliavini, F., Santana, I., Ducharme, S., Butler, C., Gerhard, A., Levin, J., Danek, A., Otto, M., Sorbi, S., Williams, S.C.R., Alexander, D.C., Rohrer, J. D., 2021. Characterizing the clinical features and atrophy patterns of MAPT-related frontotemporal dementia with disease progression Modeling. Neurology 97, e941–e952.

Zhou, C., Wang, L., Cheng, W., Lv, J., Guan, X., Guo, T., Wu, J., Zhang, W., Gao, T., Liu, X., Bai, X., Wu, H., Cao, Z., Gu, L., Chen, J., Wen, J., Huang, P., Xu, X., Zhang, B., Feng, J., Zhang, M., 2023. Two distinct trajectories of clinical and neurodegeneration events in Parkinson's disease. NPJ Parkinsons Dis 9, 111.